A Spectrally Accurate Integral Equation Solver for Molecular Surface Electrostatics

Shih-Hsien Kuo
Department of Electrical Engineering and Computer Science
Massachusetts Institute of Technology
77 Massachusetts Ave, Cambridge, MA 02139
skuo@mit.edu

Jacob White
Department of Electrical Engineering and Computer Science
Massachusetts Institute of Technology
77 Massachusetts Ave, Cambridge, MA 02139
white@mit.edu

ABSTRACT

Electrostatic analysis of complicated molecular surfaces arises in a number of nanotechnology applications including: biomolecule design, carbon nanotube simulation, and molecular electron transport. Molecular surfaces are typically smooth, without the corners common in electrical interconnect problems, and are candidates for methods with higher order convergence than that of the commonly used flat panel methods. In this paper we describe and demonstrate a spectrally accurate approach for analyzing molecular surfaces described by a collection of surface points. The method is a synthesis of several techniques, and starts by using least squares to fit a high order spherical harmonic surface representation to the given points. Then this analytic representation is used to construct a differentiable map from the molecular suface to a cube, an orthogonal basis is generated on the rectangular cube surfaces, and a change of variables is used to desingularize the required integrals of products of basis functions and Green's function. Finally, an efficient method for solving the discretized system using a matrix-implicit scheme is described. The combined method is demonstrated on an analytically solvable sphere problem, capacitance calculation of complicated molecular surface, and a coupled Poisson/Poisson-Boltzmann problem associated with a biomolecule. The results demonstrate that for a tolerance of 10^{-3} this new approach requires one to two orders of magnitude fewer unknowns than a flat panel method.

1. INTRODUCTION

When boundary element methods [15, 16] are used to solve Laplace or Helmholtz problems associated with complicated three-dimensional geometries, the associated integral equation is typically discretized using a piecewise constant basis, and a system of equations is generated using either a Galerkin or a collocation scheme. The resulting matrix equation is solved iteratively with matrix sparsification techniques [4, 13, 14, 20, 30, 32, 35]. This approach has become the method of choice for exterior problems and is used in diverse applications such as interconnect extraction [46], MEMS and fluidic simulation [33, 41], as well as in calculating bimolecular solvation energy [5, 6, 21, 45]. However, piecewise-constant bases are low order, and therefore large numbers of unknowns are needed to achieve high accuracy. While acceleration techniques make it possible to solve such problems, memory is often a bottleneck. Therefore, there is much interest in developing higher order methods [8,19,26] that can achieve faster convergence and reduce problem size. In [9, 26], the use of a higher order basis based on B-splines resulted in faster *algebraic* convergence, while in [8, 19], the aim was to attain *spectral* convergence. In this paper, we propose a new kind of higher order basis and demonstrate spectral convergence (error decays exponentially with number of unknowns). Our method differs from [8, 19] in that we use an explicit high order basis in our approach.

In simulation of molecular surface electrostatics, such as in biomolecule analysis, it is common to adopt a mixed discrete-continuum approach based on combining a continuum description of the macromolecule and solvent with a discrete description of the atomic charges [17, 25, 38, 39, 42]. In this model the interior of a molecule is approximated as a collection of point charges in a uniform dielectric material, and any surrounding solvent is modeled as a much higher permittivity electrolyte whose behavior is described by the Debye-Hückel theory. The electrostatic potential in the solvent satisfies a nonlinear Poisson-Boltzmann equation, although the simpler linearized Poisson-Boltzmann equation is more commonly solved. Integral formulations for the linearized Poisson-Boltzmann equations have been developed [5, 6, 18, 21, 43–45] for the biomolecule solvation problem, which can be used for energy calculation given a triangulation of molecular surface.

The molecular surface [10, 34], which defines an interface between a given molecule and the surrounding solvent, determines how close the solvent molecules can approach a given molecule. One common approach for constructing such a surface is to assume that a molecule is made up of atoms represented as solid spheres, and a probe sphere representing water molecules can trace out such a surface as it rolls over the union of those solid spheres. The molecular surface is thus typically made up of three analytical shapes: a spherical triangle defined by the reentrant surface of the probe when it is in simultaneous contact with three atoms, part of a torus defined by the reentrant surface of the probe when it is in simultaneous contact with two atoms, and part of spherical atoms where the probe comes into contact. Software programs [37] are available for triangulating molecular surfaces. However, in order to achieve spectral accuracy, a more accurate representation of the geometry is needed. Depending on the desired accuracy, flat panels may not be a satisfactory or efficient representation of the molecule geometry which is smooth but non-planar. In addition, as will be made clear in Section 3, in order to apply the spectral method, a mapping function is needed to describe the geometry. In the fol-

ICCAD'06 November 5-9, 2006, San Jose, CA

lowing Section, we will propose an algorithm to generate a global representation of molecular geometry that will work well with our method. We will describe the spectral method in Section 3 and discuss implementation details in Section 4. Computational results are given in Section5 and finally, we conclude in Section 6.

2. SPHERICAL HARMONIC REPRESENTATION

Molecular surface representation by spherical harmonics has been proposed by various authors [7, 11, 23, 24, 27, 28]. In such approach, a set of coefficients is generated from a point distribution or triangulation of a molecular surface, typically obtained from another program such as MSMS [37]. The coefficients, together with spherical harmonic basis, represent an analytical approximation to the surface geometry and can be differentiated. The simplest strategy for generating the spherical harmonic representation is to first pick a "molecular center" to be the origin of a spherical coordinate system, and then represent each surface point using a spherical harmonic expansion as

$$r(\theta,\phi) \approx \sum_{n=0}^{N} \sum_{m=-n}^{n} c_n^m Y_n^m(\theta,\phi) \tag{1}$$

where N is the expansion order, r, θ and ϕ are the spherical coordinates of points on the surface.

$$Y_n^m(\theta,\phi) = \begin{cases} \alpha_n^m P_n^m(cos\theta)\cos m\phi & \text{if } m \geq 0 \\ \alpha_n^{|m|} P_n^{|m|}(cos\theta)\sin |m|\phi & \text{if } m < 0 \end{cases} \tag{2}$$

where $P_n^m(\theta,\phi)$ are associated Legendre functions, and

$$\alpha_n^m = (-1)^m \sqrt{\frac{(2-\delta_{0m})(2n+1)}{4\pi}\frac{(n-m)!}{(n+m)!}} \tag{3}$$

are normalization constants chosen such that the basis are orthonormal. It does have the limitation that the surface has to be starlike [11], which means that there exists an origin within the molecule such that an outgoing ray intersects the molecular surface exactly once. Other techniques that avoid this restriction are available [7, 11, 23] for surfaces that are topologically equivalent to a sphere.

The coefficients c_n^m can be calculated by forming the inner product integral of $r(\theta,\phi)$ with a spherical harmonic basis. Instead, we adopt a more easily implemented least squares approach [7]. Given a set of k points (r,θ,ϕ) on a molecular surface, we look for a set of coefficients $\{a_j\} = \{c_n^m\}$ such that $||r - Aa||_2$ is minimized, where each element of A are spherical harmonics evaluated at (θ,ϕ) coordinates:

$$A_{i,j} = A_{i,n^2+m+n+1} = Y_n^m(\theta_i,\phi_i) \tag{4}$$

for $1 \leq i \leq k$ and $1 \leq j \leq (N+1)^2$. To solve the least-squares problem, we used the singular value decomposition, $A = U\Sigma V^T$ [40]. The set of coefficients in (1) can then be obtained from

$$a = V\Sigma^{-1}U^T r \tag{5}$$

where $a_j = a_{n^2+m+n+1} = c_n^m$.

3. SPECTRAL METHOD

The following integral equation will be used as our model problem:

$$\phi(\vec{r}) = \int_\Omega G(\vec{r},\vec{r}')\sigma(\vec{r}')\,dS' \tag{6}$$

where Ω is the surface boundary of a three-dimensional region of interest on which we would like to solve for the unknown quantity σ given an arbitrary ϕ. The Green's function $G(\vec{r},\vec{r}')$ can take the following forms:

$$G(\vec{r},\vec{r}') = \frac{1}{r}, \frac{e^{-\kappa r}}{r} \qquad \kappa \in \mathbf{R} \tag{7}$$

where $r = |\vec{r} - \vec{r}'|$ is the Euclidean distance between a source and target point. In traditional panel method, a triangular mesh is commonly used to discretize the geometry, and a basis set, $\{B_i : i = 1,2,\ldots,n\}$, is usually defined on the same mesh, with B_i's being non-zero only on a few triangles.

The basis is used to discretize the unknown as in

$$\sigma(\vec{r}) = \sum_{i=1}^{n} \sigma_i B_i(\vec{r}) \tag{8}$$

where σ_i's are the corresponding weights which are solution of the discretized problem. An alternative basis for discretization is a set of numerically orthogonal polynomials defined by carefully chosen quadrature points. In contrast to a panel-based representation whereby orthogonality is only partially maintained by spatial separation of bases' supports, a quadrature based approach ensures good orthogonality for arbitrarily high order bases, though their supports have significant overlap. The improvement in accuracy is significant: quadrature-based methods exhibit a spectral convergence rates. In this section, we will describe the basis, the techniques for integration over curved surfaces, and other features associated with this approach.

3.1 Numerically Orthogonal Basis

Consider a global surface Ω of coordinates (x,y,z) that can be partitioned into a few regions and each of which can be associated with a one-to-one mapping function:

$$P : \vec{r}_{flat}(u,v) \rightarrow \vec{r}_{curve}(x,y,z) \tag{9}$$

defined on a local patch of coordinates (u,v). In a complicated geometry where exact mapping is not possible, a high order approximation, consistent with the basis order, has to be used since convergence is limited by the lower accuracy of the two. A second requirement is the availability of good quadrature points associated with each patch. For example, in a rectangular patch a tensor product of one-dimensional Gauss-Lobatto quadrature points is used, and basis set can be similarly defined as polynomials that take on unit value at one of the grid points but zero at all other grid points. In one dimension, these are the Lagrangian interpolating polynomials [3]:

$$\ell_i(u) = \frac{\prod_{k=1,k\neq i}^{m}(u-u_k)}{\prod_{k=1,k\neq i}^{m}(u_i-u_k)} \tag{10}$$

such that

$$\ell_i(u_k) = \delta_{ik} \qquad i,k = 1,\ldots,m \tag{11}$$

where u_k is coordinate of kth quadrature point. The bases on a patch can therefore be written as a product of two one-dimensional polynomials as in

$$B_{(i*j)}(u,v) = \ell_i(u)\ell_j(v). \tag{12}$$

Therefore, if m quadrature points are used along each dimension, there will be m^2 basis functions. A good set of quadrature points

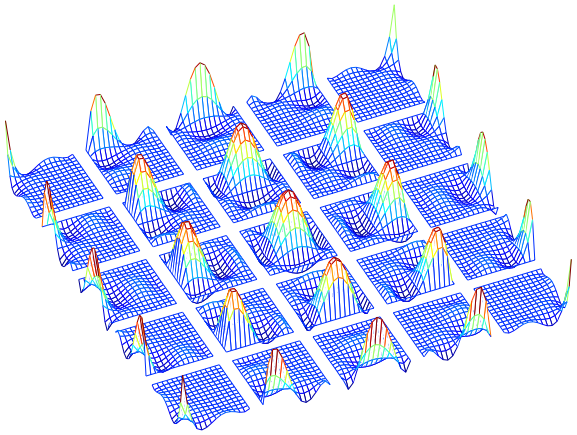

Figure 1: Two-dimensional lagrangian basis defined by 5×5 Gauss-Lobatto grid on a patch.

ensures orthogonality as the inner product over a patch approximated by the same quadrature points is always zero by design. Fig. 1 shows such a set of basis defined on a patch. Each of the 25 basis takes on unit value at one of the Gauss-Lobatto grid points, and are zero at all other grid points. For the bases associated with a boundary node, the support will span across nearby patches so that computed solutions will be continuous along patch boundaries. The use of such a numerically orthogonal basis was proposed in the spectral element method [31] and is well known in the finite element community. However, to authors' knowledge, it has not yet been applied to the boundary element method, perhaps hindered by the difficulty of panel integration, the subject of the next section.

3.2 Integration over Curved Surfaces

Once the mapping function (9) and basis functions (12) have been defined on a patch, integration of products of Green's and basis functions over the actual surface can be performed using parametric coordinates (u,v). For an evaluation point at $\vec{r}(x,y,z)$:

$$\int\limits_{(x,y,z)} G(\vec{r},\vec{r}')B_i(\vec{r}')\,dS' = \int\limits_{(u,v)} G(\vec{r},P(\vec{r_f}'))B_i(\vec{r_f}')|J(\vec{r_f}')|\,dS' \quad (13)$$

where $\vec{r_f}'$ is such that $P(\vec{r_f}') = \vec{r}'$ (see (9)), $|J|$ is the Jacobian of the mapping function P. Note that the basis function, originally defined on the local patch, is also being used to represent the solution in the global surface through the mapping function:

$$B_i(\vec{r}'(x,y,z)) = B_i(P(\vec{r_f}'(u,v))). \quad (14)$$

An analytical expression for (13) is not generally available as the Jacobian can be very complicated, and straightforward quadrature in (u,v) coordinates is not sufficiently accurate for evaluation points on or close to the surface associated with a source patch. It is shown in [8] that, however, the integral can be de-singularized in appropriately chosen polar coordinates in place of u and v. The key is to locate the polar coordinates origin such that the radial coordinate ρ goes to zero at the singular point. The resulting integrand is smooth and can be evaluated using Gauss quadrature points in (ρ,ϑ). In particular, if the evaluation point $\vec{r}_j$ is such that $P^{-1}(\vec{r}_j)$ is on the patch, then

$$(u_o,v_o) = P^{-1}(\vec{r}_j(x,y,z)) \quad (15)$$

and

$$\begin{aligned} u-u_o &= \rho\cos\vartheta \\ v-v_o &= \rho sin\vartheta \end{aligned}. \quad (16)$$

is the appropriate change of variables to apply to (13).

3.3 Jacobian of Spherical Harmonic Surface

In order to incorporate the spherical harmonic representation into the spectral method, one must be able to integrate over the molecular surface given by (1). In addition, in order to de-singularize the integral involving the Green's function, our approach is to carry out the integration patch-wise on six faces of a cube by setting up appropriate polar coordinates on each face. Consider the area integral in order to figure out the appropriate Jacobian. Given a molecular surface parameterized by θ and ϕ, the normal vector is given by:

$$\hat{N} = \frac{\vec{R}_\theta \times \vec{R}_\phi}{|\vec{R}_\theta \times \vec{R}_\phi|} \quad (17)$$

and the area integral is given by:

$$\int dS = \int_0^{2\pi}\int_0^{\pi} |\vec{R}_\theta \times \vec{R}_\phi|\,d\theta\,d\phi \quad (18)$$

where

$$\vec{R} = r(\theta,\phi)\sin\theta\cos\phi\hat{x} + r(\theta,\phi)\sin\theta\sin\phi\hat{y} + r(\theta,\phi)\cos\theta\hat{z} \quad (19)$$

is position vector of any point on the molecular surface, $\vec{R}_\theta$ and $\vec{R}_\phi$ are the partial derivative of $\vec{R}$ with respect to θ and ϕ respectively. Alternatively, the cross product in (18) can be expressed in spherical coordinates [1, 12]:

$$\vec{R}_\theta \times \vec{R}_\phi = r^2\sin\theta\hat{r} - rr_\theta\sin\theta\hat{\theta} - rr_\phi\hat{\phi} \quad (20)$$

so that

$$\int dS = \int_0^{2\pi}\int_0^{\pi} r\sqrt{r^2\sin^2\theta + r_\theta^2\sin^2\theta + r_\phi^2}\,d\theta\,d\phi \quad (21)$$

where $r = r(\theta,\phi)$ in (1), r_θ and r_ϕ are derivatives of radius coordinate with respect to θ and ϕ respectively.

In order to carry out the surface integral on a reference patch on each face of a cube, one needs the Jacobian for the change of variables:

$$d\theta\,d\phi = |J_{map}|\,du\,dv \quad (22)$$

which corresponds to a mapping from a flat surface parameterized by (u,v) to angular coordinates (θ,ϕ). Consider the sphere example where $r = r_o$ is constant so that

$$\int\limits_{sphere} dS = \int_0^{2\pi}\int_0^{\pi} r_o^2\sin\theta\,d\theta\,d\phi = \iint\limits_{cube} \frac{hr_o^2}{(u^2+v^2+h^2)^{3/2}}\,du\,dv \quad (23)$$

where h is perpendicular distance from center of sphere to a cube face, one can deduce that

$$|J_{map}| = \frac{h}{\sin\theta(u^2+v^2+h^2)^{3/2}} \quad (24)$$

when mapping is along radial direction from center of cube which coincides with center of sphere. We are now in a position to carry out surface integral on reference patches of a cube by combining equations (21), (22) and (24) where radius function in (1) is represented by spherical harmonics. The evaluation of r and r_ϕ is according to the definition of real spherical harmonics in (2) and r_θ can be calculated using the following relation:

$$\frac{dP_n^m(\cos\theta)}{d\theta} = \frac{(n-|m|+1)P_{n+1}^{|m|} - (n+1)\cos\theta P_n^{|m|}}{\sin\theta}. \quad (25)$$

Therefore, when spherical harmonics are used to represent a smooth surface, the Jacobian in (13) is given by

$$|J| = |\overrightarrow{R}_\theta \times \overrightarrow{R}_\phi||J_{map}|. \tag{26}$$

4. IMPLEMENTATION DETAILS

4.1 Iterative Solver

The cost of constructing the collocation matrix in (**??**) depends on the number of quadrature points used in the polar coordinates. And the use of higher order basis requires a similarly higher order quadrature scheme in order to accurately approximate the integral. In our implementation, if $m \times m$ grid points are used in a local patch, each basis will be a two-dimensional polynomial of degree $m-1$ in each of (u,v) coordinates, a Gauss quadrature scheme of similar order in polar coordinates (ρ,ϑ) is used. Thus there are $O(m^2)$ quadrature points per patch associated with each matrix entry, and this tends to dominate the computation time. Since many bases share their supports on a patch, an efficient implementation should recycle quadrature points defined on (ρ,ϑ) among them. This is most easily implemented by an iterative solver approach:

$$\begin{aligned}
\phi(\vec{r}_j) &= \sum_{i=1}^{n} A_{ji}^{Collocation}\sigma_i \\
&= \sum_{i=1}^{n} \sigma_i \left(\iint G(\vec{r}_j,\rho,\vartheta) B_i(\rho,\vartheta) |J(\rho,\vartheta)| \, \rho \, d\rho \, d\vartheta \right) \qquad (27) \\
&= \iint G(\vec{r}_j,\rho,\vartheta) \left(\sum_{i=1}^{n} \sigma_i B_i(\rho,\vartheta) \right) |J(\rho,\vartheta)| \, \rho \, d\rho \, d\vartheta \qquad (28)
\end{aligned}$$

where $\sigma_i = \sigma(\vec{r}_i)$ is test solution at collocation points. The summation over all patches within a basis' support is implicity assumed here. As opposed to an direct solver whereby integration over patches is done for individual basis functions in (27), at each iteration step, a weighted sum of all bases in (28) is integrated instead. This is equivalent to first interpolating on each patch via a set of Gauss-Lobatto points, then integrating the interpolated function over the corresponding global surface. In addition to the computing efficiency, an iterative solver uses less memory than than a direct solver so larger problems may be solved.

4.2 Algorithm Steps

Below we give a summary of all the steps involved in the matrix-vector multiplication used in an iterative solver. We will assume that a spherical harmonic representation of geometry has been obtained, and the basis set is defined using Gauss-Lobatto grids on each face of a cube. Given σ_i at collocation points, potentials at evaluation points can be computed as follows:

```
for each evaluation point
  for each patch
```

1. Choose origin of polar coordinates on a patch according to (15), if evaluation point is on patch. Otherwise, choose the nearest point on patch as the origin.
2. Partition patch into triangles by connecting the origin to all vertices. Set up quadrature points in polar coordinates for each triangle.
3. Evaluate basis at quadrature points by (10) and (12). The interpolated function at quadrature points are given by (8).
4. Evaluate Jacobian at quadrature points by (26), (24), (20) and (1).
5. Evaluate Green's function at quadrature points via projection of quadrature points according to (19) and (1).
6. Integrate on a reference triangle using the above functional evaluations at quadrature points and appropriate quadrature weights.
7. Calculate the integral on a patch in (28) by summing up contribution from each triangle.

```
  end
end
```

5. COMPUTATIONAL RESULTS

5.1 Potential Flow On Sphere

A unit sphere in an infinite fluid potential flow problem, which has an analytical solution [29, 32] is used to validate the proposed approach. The integral equation in this case is

$$\phi(\vec{r}) = \int \frac{\sigma(\vec{r}')}{|\vec{r}-\vec{r}'|} \, dS'. \tag{29}$$

where $\phi(\vec{r})$ is given. The spherical geometry can be easily described by a mapping function that radially project any point on a cube to sphere. The Jacobian of the mapping is given in (24). An $m \times m$ Gauss-Lobatto grid is used on each face of a cube, a basis set is defined on the grid and $2m \times 2m$ quadrature points in polar coordinates are used to evaluate the integral in (27) or (28).

Accuracy is assessed in terms of integrated error, which is the sum of errors at collocation points, normalized by area. Fig. 2 shows the spectral convergence results and a comparison to the standard panel method. Results obtained from a direct solver using Gaussian elimination and an iterative solver using GMRES [36] are also shown. It can be seen that both direct and iterative solution show similar convergence behavior: a straight line in a log-linear plot and a curve in a log-log plot indicates spectral convergence, and the error decays exponentially with number of unknowns.

As shown in Fig. 2(b), the improvement over the traditional approach is clear: not only is the accuracy better for the same number of degrees of freedom, or fewer unknowns are needed for the same accuracy, but the method's advantage grows with increasing problem size or more stringent error tolerance. For the sphere problem, the spectral method is able to achieve six digits of accuracy with about 500 unknowns. By extrapolating the straight line, one can estimate that at least a million panels are needed for the standard method to achieve the same accuracy.

5.2 Capacitance of a Spherical Harmonic Surface

In order to verify the above method for a general molecular surface, we use the example of a small organic molecule with 26 atoms, the transition state analog (TSA) of the protein enzyme chorismate mutase. The geometry of this small molecule was taken directly from an X-ray crystal structure [22], and can be obtained from the Protein Data Bank (PDB) [2] as accession number 1ECM. The radii used were 1.0 Å for hydrogens, 1.4 Å for oxygens, 2.0 Å for aliphatic carbons, and 1.7 Å for carbonyl or vinyl carbons. The surface of the TSA molecule was triangulated with the program MSMS [37], using a probe radius of 1.4 Å for water. A spherical harmonic representation is obtained by least squares fit to vertices of the triangulation. Fig. 3 shows an order 10 approximation with

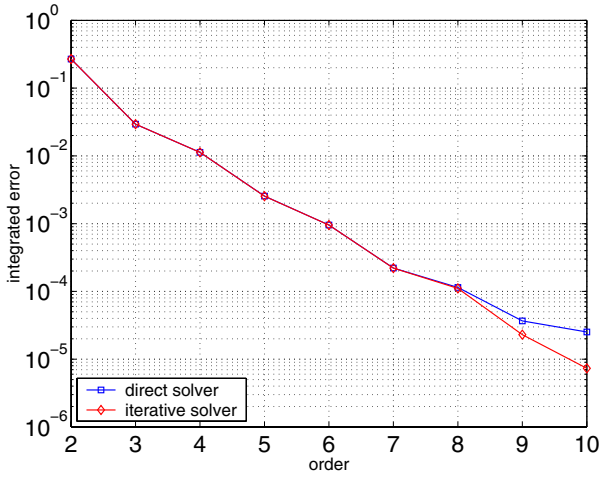

(a) log-linear scale

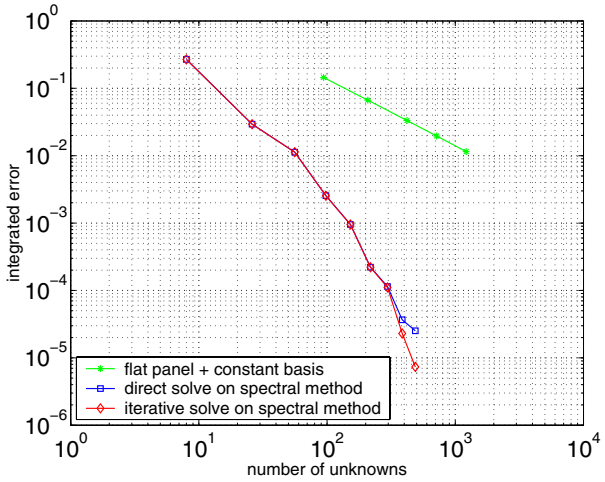

(b) log-log scale

Figure 2: Accuracy comparison between the standard and spectral method.

121 coefficients for the surface using 3359 points, and a triangulation of 6714 panels. The color in the spherical harmonic surface correspond to the radial distance from the center of expansion, while the color in the triangulated surface correspond to the torireentrant, spherical-reentrant and contact surface in the definition of molecular surface. The area of a spherical harmonic surface can be calculated using (21), and is compared to analytical area given by MSMS for increasing order of approximation. In Fig. 4, the area convergence versus number of coefficients is shown for three sets of point distributions. The data demonstrated that 5 to 10 times as many points as coefficients can generate a reasonable approximation. For the order 10 expansion, the area approximation incurs less than 0.3% relative error.

Once a spherical harmonic surface is obtained, we can apply the spectral method to solve the integral equation in (29), where for the capacitance problem, the potential is set to unity. We can therefore compare our method to the standard panel method implemented in FastCap [30]. The spherical harmonic surface in Fig. 3(a) is used for geometrical representation in the spectral method, and triangulation from MSMS is used to generate input files for the FastCap program. The capacitance calculation for the two solvers

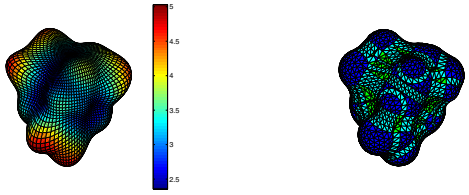

(a) harmonic expansion (b) triangulation

Figure 3: Spherical harmonic approximation of a triangulated molecular surface.

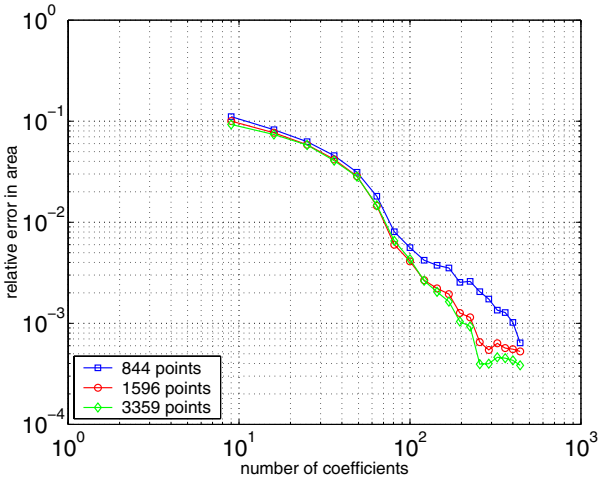

Figure 4: Area convergence of spherical harmonic approximation.

with increasing discretization is shown in Fig. 5. For the spectral method, the number of unknowns correspond to number of global lagrangian basis used while for the standard panel method, the number of unknowns correspond to number of panels in the triangulation. For the spectral method, the result converges to three significant figures with 386 unknowns while in the standard method, the same convergence can only be achieved with 27742 unknowns. The spectral method requires almost two orders of magnitude fewer unknowns for a tolerance of 10^{-3}, which is consistent with the sphere example.

5.3 Solvation Energy of a Biomolecule

For the same TSA molecule, we would like to calculate the solvation energy when the molecule is in an ionic solution. We use the formulation in [21] to obtain a solution of a linearized Poisson-Boltzmann equation. The coupled integral equations of interest are:

$$\frac{1}{2}\varphi_1(\vec{r}_o) + \int_\Omega \left[\varphi_1(\vec{r}')\frac{\partial G_1}{\partial n}(\vec{r}_o;\vec{r}') - G_1(\vec{r}_o;\vec{r}')\frac{\partial \varphi_1}{\partial n}(\vec{r}')\right] d\vec{r}' = \sum_{i=1}^{n_c} \frac{q_i}{\varepsilon_1} G_1(\vec{r}_o;\vec{r}_i) \quad (30)$$

and

$$\frac{1}{2}\varphi_1(\vec{r}_o) + \int_\Omega \left[-\varphi_1(\vec{r}')\frac{\partial G_2}{\partial n}(\vec{r}_o;\vec{r}') + G_2(\vec{r}_o;\vec{r}')\frac{1}{\varepsilon}\frac{\partial \varphi_1}{\partial n}(\vec{r}')\right] d\vec{r}' = 0 \quad (31)$$

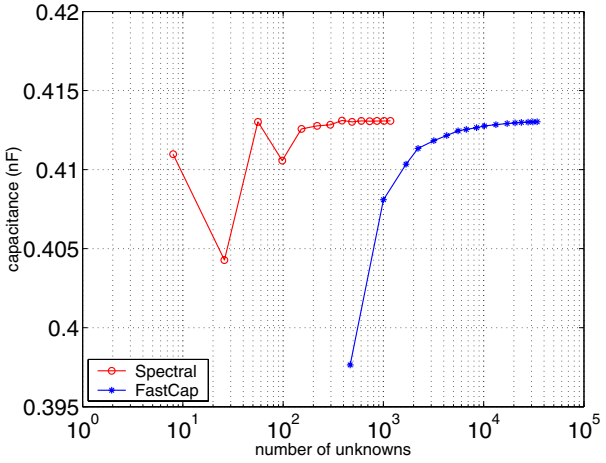

Figure 5: Capacitance calculation of the TSA molecule.

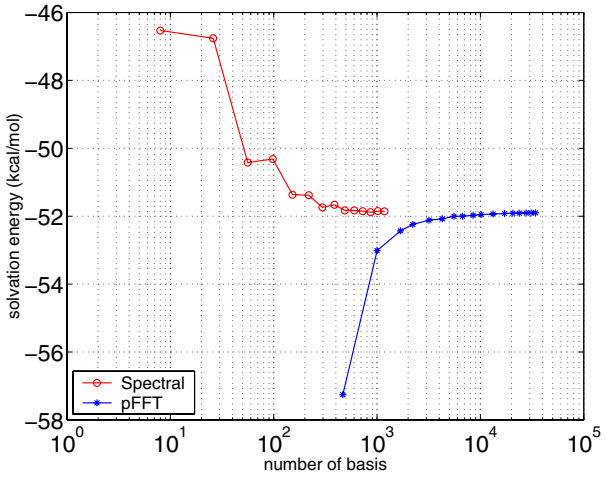

Figure 6: Solvation energy calculation of the TSA molecule.

where the unknown quantities are potential φ_1 at the dielectric interface and its normal derivative $\frac{\partial \varphi_1}{\partial n}$ on the inner surface. The normal derivative at the interface has a jump that is related to the relative dielectric constant ε. The free charges, q_i, are derived from quantum mechanical calculations. The Green's functions are:

$$G_1(\vec{r};\vec{r}') = \frac{1}{4\pi|\vec{r}-\vec{r}'|} \quad (32)$$

$$G_2(\vec{r};\vec{r}') = \frac{e^{-\kappa|\vec{r}-\vec{r}'|}}{4\pi|\vec{r}-\vec{r}'|} \quad (33)$$

where $\kappa = 0.124$ Å^{-1}, equivalent to an ionic strength of 0.145 M at 25° C was used. A dielectric constant of 4 ε_0 was used inside the TSA molecule and a dielectric of 80 ε_0 was used externally. Once the potential and its normal derivative are computed on the molecular surface, potentials everywhere can be calculated. In particular, the potential at each charge location, known as the reaction potential, is given by

$$\varphi^{REAC}(\vec{r}_i) = \int_\Omega \left[G_1(\vec{r}_i;\vec{r}')\frac{\partial \varphi_1}{\partial n}(\vec{r}') - \varphi_1(\vec{r}')\frac{\partial G_1}{\partial n}(\vec{r}_i;\vec{r}') \right] d\vec{r}'. \quad (34)$$

The solvation energy can be calculated by multiplying these potentials with corresponding charge magnitudes.

The spectral method is again compared with the standard panel method implemented with precorredted-FFT acceleration [21, 32, 46]. The results are shown in Fig. 6. Note that the size of matrix equation is twice the size of the basis set shown on the x-axis, since there are two sets of unknowns in the coupled integral equations. This problem is also more challenging due to the presence of double layer potentials. To converge to three significant figures, the spectral method requires 488 basis functions while 8502 panels are needed, a factor of 20 improvement.

6. CONCLUSION

This paper describes a novel approach to discretizing integral equations with singular kernels, such as those associated with electrostatic analysis of molecular surfaces. A spherical harmonic analytic representation of the surface is generated and used to construct a mapping from local patches to the surface, and a global, numerically orthogonal basis is defined on local patches and used to represent the solution. Integration on a patch is done by quadrature in carefully chosen polar coordinates. In an iterative solver implementation, integration over a patch by quadrature only needs to be done once per evaluation point. Therefore, our approach can be very efficient as number of patches is small and kept constant as the basis size increases. Computational results demonstrate the method is capable of achieving spectral convergence. In comparison to the standard panel method, our approach requires many fewer unknowns for a given accuracy.

While in the panel method, both geometrical discretization and basis supports are defined on a mesh, they are decoupled in the proposed spectral method. On the other hand, mapping functions are required to describe the geometry. In simulation of molecular electrostatics, spherical harmonics can be a good candidate for representing molecular surfaces, but work is needed to generalize the mapping to more irregular molecules.

7. ACKNOWLEDGMENT

The authors acknowledge the support of the MIT-SMA System Biology and BioMEMS programs, the NIH ICBP project, and the National Science Foundation. The authors would also like to thank Michael Altman, Jay Bardhan and Bruce Tidor for helpful discussions and for providing a software program and examples which were used in some of the comparisons.

8. REFERENCES

[1] A. Baxansky and N. Kiryati. Calculating geometric properties of three-dimensional objects from the spherical harmonic representation. Technical Report VIA-2005-6-1, Tel Aviv University, June 2005.

[2] H. M. Berman, J. Westbrook, Z. Feng, G. Gilliland, T. N. Bhat, H. Weissig, I. N. Shindyalov, and P. E. Bourne. The Protein Data Bank. *Nucleic Acids Research*, 28(1):235–242, 2000.

[3] J.-P. Berrut and L. N. Trefethen. Barycentric lagrange interpolation. *SIAM Review*, 46(3):501–517, 2004.

[4] G. Beylkin, R. Coifman, and V. Rokhlin. Fast wavelet transforms and numerical algorithms I. *Communications on Pure and Applied Mathematics*, 44:141–183, 1991.

[5] R. Bharadwaj, A. Windemuth, S. Sridharan, B. Honig, and A. Nicholls. The fast multipole boundary element method for molecular electrostatics: An optimal approach for large

systems. *Journal of Computational Chemistry*, 16:898–913, 1995.

[6] A. Boschitsch, M. Fenley, and H.-X. Zhou. Fast boundary element method for the linear poisson-boltzmann equation. *Journal of Physical Chemistry B*, 106(10):2741–2754, 2002.

[7] C. Brechbühler, G. Gerig, and O. Kübler. Parametrization of closed surfaces for 3-D shape description. *Computer Vision and Image Understanding*, 61(2):154–170, 1995.

[8] O. Bruno and L. Kunyansky. A fast, high-order algorithm for the solution of surface scattering problems: basic implementation, tests, and applications. *Journal of Computational Physics*, 169(1):80–110, 2001.

[9] B. Büchmann. Accuracy and stability of a set of free-surface time-domain boundary element models based on B-splines. *International Journal for Numerical Methods in Fluids*, 33(1):125–155, 2000.

[10] M. L. Connolly. Analytical molecular surface calculation. *Journal of Applied Crystallography*, 16:548–558, 1983.

[11] B. S. Duncan and A. J. Olson. Approximation and characterization of molecular surfaces. *Biopolymers*, 33(2):219–229, Feb. 1993.

[12] E. J. Garboczi. Three-dimensional mathematical analysis of particle shape using x-ray tomography and spherical harmonics: Application to aggregates used in concrete. *Cement and Concrete Research*, 32(10):1621–1638, Oct. 2002.

[13] L. Greengard. *The Rapid Evaluation of Potential Fields in Particle Systems*. MIT Press, 1988.

[14] W. Hackbusch and Z. P. Nowak. On the fast matrix multiplication in the boundary element method by panel clustering. *Numerische Mathematik*, 54:463–491, 1989.

[15] R. F. Harrington. *Field Computation by Moment Methods*. MacMillan, 1968.

[16] J. L. Hess and A. M. O. Smith. Calculation of nonlifting potential flow about arbitrary three-dimensional bodies. *Journal of Ship Research*, 8(2):22–44, 1964.

[17] B. Honig and A. Nicholls. Classical electrostatics in biology and chemistry. *Science*, 268:1144–1149, 1995.

[18] A. H. Juffer, E. F. F. Botta, B. A. M. V. Keulen, A. V. D. Ploeg, and H. J. C. Berendsen. The electric potential of a macromolecule in a solvent: A fundamental approach. *Journal of Computational Physics*, 97:144–171, 1991.

[19] S. Kapur and D. Long. High-order Nyström schemes for efficient 3-D capacitance extraction. In *Proceedings of the International Conference on Computer-Aided Design*, pages 178–185, 1998.

[20] S. Kapur and D. E. Long. IES^3: A fast integral equation solver for efficient 3-dimensional extraction. In *Proceedings of the International Conference on Computer-Aided Design*, pages 448–455, San Jose, CA, 1997.

[21] S. S. Kuo, M. D. Altman, J. P. Bardhan, B. Tidor, and J. K. White. Fast methods for simulation of biomolecule electrostatics. In *Proceedings of the International Conference on Computer-Aided Design*, San Jose, CA, Nov. 2002.

[22] A. Y. Lee, P. A. Karplus, B. Ganem, and J. Clardy. Atomic structure of the buried catalytic pocket of escherichia coli chorismate mutase. *Journal of the American Chemical Society*, 117(12):3627 – 3628, 1995.

[23] S. Leicester, J. Finney, and R. Bywater. A quantitative representation of molecular surface shape. i: Theory and development of the method. *Journal of Mathematical Chemistry*, 16:315–341, 1994.

[24] S. E. Leicester, J. L. Finney, and R. P. Bywater. Description of molecular surface shape using fourier descriptors. *Journal of Molecular Graphics*, 6(2):104–108, 1988.

[25] J. D. Madura, J. M. Briggs, R. C. Wade, M. E. Davis, B. A. Luty, A. Ilin, J. Antosiewicz, M. K. Gilson, B. Bagheri, L. Ridgway-Scott, and J. A. McCammon. Electrostatics and diffusion of molecules in solution: Simulations with the University of Houston Brownian Dynamics program. *Computer Physics Communications*, 91:57–95, 1995.

[26] H. D. Manier. *A Three Dimensional Higher Order Panel Method based on B-splines*. PhD thesis, Massachusetts Institute of Technology, Cambridge, MA, 1995.

[27] N. L. Max and E. D. Getzoff. Spherical harmonic molecular surfaces. *IEEE Computer Graphics and Applications*, 8(4):42–50, 1988.

[28] R. J. Morris, R. J. Najmanovich, A. Kahraman, and J. M. Thornton. Real spherical harmonic expansion coefficients as 3D shape descriptors for protein binding pocket and ligand comparisons. *Bioinformatics*, 21(10):2347–2355, Feb. 2005.

[29] K. Nabors, F. T. Korsmeyer, F. T. Leighton, and J. White. Preconditioned, adaptive, multipole-accelerated iterative methods for three-dimensional first-kind integral equations of potential theory. *SIAM Journal on Scientific Computing*, 15(3):713–735, 1994.

[30] K. Nabors and J. White. FastCap: A multipole accelerated 3-D capacitance extraction program. *IEEE Transactions on Computer-Aided Design*, 10(11):1447–1459, Nov. 1991.

[31] A. T. Patera. A spectral element method for fluid dynamics: Laminar flow in a channel expansion. *Journal of Computational Physics*, 54:468–488, June 1984.

[32] J. R. Phillips and J. K. White. A precorrected-FFT method for electrostatic analysis of complicated 3-D structures. *IEEE Transactions on Computer-Aided Design*, 16(10):1059–1072, Oct. 1997.

[33] D. Ramaswamy, W. Ye, X. Wang, and J. White. Fast algorithms for 3-D simulation. *Journal of Modeling and Simulation of Microsystems*, 1(1):77–82, Dec. 1999.

[34] F. M. Richards. Areas, volumes, packing, and protein structure. *Annual Review of Biophysics and Bioengineering*, 6:151–176, 1977.

[35] V. Rokhlin. Rapid solution of integral equations of classical potential theory. *Journal of Computational Physics*, 60:187–207, 1985.

[36] Y. Saad and M. Schultz. GMRES: A generalized minimal residual algorithm for solving nonsymmetric linear systems. *SIAM Journal of Scientific and Statistical Computing*, 7:856–869, 1986.

[37] M. Sanner, A. J. Olson, and J. C. Spehner. Reduced surface: An efficient way to compute molecular surfaces. *Biopolymers*, 38:305–320, 1996.

[38] K. A. Sharp and B. Honig. Electrostatic interactions in macromolecules: Theory and applications. *Annual Review of Biophysics and Biophysical Chemistry*, 19:301–332, 1990.

[39] C. Tanford and J. G. Kirkwood. Theory of protein titration curves I. general equations for impenetrable spheres. *Journal of the American Chemical Society*, 59:5333–5339, 1957.

[40] L. N. Trefethen and D. Bau, III. *Numerical Linear Algebra*. Society for Industrial & Applied Mathematics, 1997.

[41] J. C. Vassberg. A fast surface-panel method capable of solving million-element problems. Aerospace Sciences Meeting and Exhibit, 35th, Reno, NV, Jan. 1997. AIAA

Paper 97-0168.

[42] J. Warwicker and H. C. Watson. Calculation of the electric potential in the active site cleft due to alpha-helix dipoles. *Journal of Molecular Biology*, 157:671–679, 1982.

[43] B. J. Yoon and A. M. Lenhoff. A boundary element method for molecular electrostatics with electrolyte effects. *Journal of Computational Chemistry*, 11:1080–1086, 1990.

[44] R. J. Zauhar and R. S. Morgan. The rigorous computation of the molecular electric potential. *Journal of Computational Chemistry*, 9:171–187, 1988.

[45] R. J. Zauhar and A. Varnek. A fast and space-efficient boundary element method for computing electrostatic and hydration effects in large molecules. *Journal of Computational Chemistry*, 17:864–877, 1996.

[46] Z. Zhu, B. Song, and J. White. Algorithms in FastImp: A fast and wideband impedance extraction program for complicated 3-D geometries. In *Proceedings of the Design Automation Conference*, pages 712 –717, Anaheim, CA, June 2003.